

1 ***Enterococcus faecalis* modulates immune activation and slows healing during**
2 **wound infection**

3

4 Running title: Mouse model for *E. faecalis* wound infection

5

6 Kelvin Kian Long Chong^{1,2,*}, Wei Hong Tay^{1,3,*}, Baptiste Janela⁴, Mei Hui Adeline

7 Yong^{1,5}, Tze Horng Liew¹, Leigh Madden⁶, Damien Keogh¹, Timothy Mark Sebastian

8 Barkham⁷, Florent Ginhoux⁴, David Laurence Becker⁶, Kimberly A. Kline^{1,4,#}

9

10 ¹Singapore Centre for Environmental Life Sciences Engineering, Nanyang

11 Technological University, SBS-B1n-27, 60 Nanyang Drive, Singapore 637551

12 ²Nanyang Institute of Technology in Health and Medicine (NITHM), Research Techno

13 Plaza, Nanyang Technological University, Frontiers Block #02-07, 50 Nanyang Drive,

14 Singapore 637553

15 ³Singapore Centre for Environmental Life Sciences Engineering, Interdisciplinary

16 Graduate School, Nanyang Technological University, SBS-B2n-27, 60 Nanyang Drive,

17 Singapore 637551

18 ⁴Singapore Immunology Network (SIgN), Agency for Science, Technology and

19 Research (A*STAR), 8A Biomedical Grove, Singapore 138648

20 ⁵School of Biological Sciences, Nanyang Technological University, SBS-B2n-27, 60

21 Nanyang Drive, Singapore 637551

22 ⁶Lee Kong Chian School of Medicine, Nanyang Technological University, 11 Mandalay
23 Road, Singapore 308232

24 ⁷Department of Laboratory Medicine, Tan Tock Seng Hospital, 11 Jalan Tan Tock Seng,
25 Singapore 308433

26 *These authors contributed equally to this work.

27 #Correspondence: kkline@ntu.edu.sg

28

29 **ABSTRACT**

30 *Enterococcus faecalis* is one of most frequently isolated bacterial species in wounds yet
31 little is known about its pathogenic mechanisms in this setting. Here, we used a mouse
32 wound excisional model to characterize the infection dynamics of *E. faecalis* and show
33 that infected wounds result in two different states depending on the initial inoculum. Low
34 dose inocula were associated with short term, low titer colonization whereas high dose
35 inocula were associated with acute bacterial replication and long term persistence. High
36 dose infection and persistence were also associated with immune cell infiltration,
37 despite suppression of some inflammatory cytokines and delayed wound healing.
38 During high dose infection, the multiple peptide resistance factor (MprF) which is
39 involved in resisting immune clearance, contributes to *E. faecalis* fitness. These results
40 comprehensively describe a mouse model for investigating *E. faecalis* wound infection
41 determinants, and suggest that both immune modulation and resistance contribute to
42 persistent, non-healing wounds.

43 (150 words – Abstract)

44 (3496 words – Main Text)

45 (49 references)

46 **Keywords**

47 *Enterococcus faecalis*, wound infections, persistence, immune evasion, multiple peptide
48 resistant factor, antimicrobial peptide, wound healing, inflammation

49 INTRODUCTION

50 Wound infections affect between 7-15% of hospitalized people globally [1]. *E. faecalis* is
51 one of the most frequently isolated bacterial species across all types of wounds,
52 including diabetic foot ulcers, burns, and surgical sites [2-4]. In surgical site infections
53 (SSIs), *E. faecalis* is the third most commonly isolated organism [5, 6]. *E. faecalis*
54 infections are increasingly difficult to treat due to their intrinsic and acquired resistance
55 to a range of antibiotics [7]. Despite the high frequency of *E. faecalis* in wound
56 infections, little is known about its pathogenic strategies in this niche.

57 Bacterial biofilms, which are often polymicrobial in nature, are a major factor in wound
58 healing [8-10]. Biofilm-associated wound infections are associated with a poorer
59 prognosis [8, 9]. Moreover, biofilm formation promotes survival and persistence of
60 infecting microbial species because it facilitates defence against the host immune
61 response [11]. *E. faecalis* encodes several factors that contribute to biofilm formation,
62 including two sortase enzymes, SrtC and SrtA, that polymerize and attach endocarditis-
63 and biofilm-associated pili (Ebp) to the cell wall, respectively [12-14]. Ebp pili aid in the
64 attachment of *E. faecalis* to surfaces, which is required in the initial stages of biofilm
65 formation *in vitro* and *in vivo* during catheter-associated urinary tract infection (CAUTI)
66 [15, 16]. Other biofilm-associated factors that are attached to the cell wall by SrtA
67 include Ace, aggregation substance, and Esp [17-20].

68 In addition to initial adhesion and colonization, *E. faecalis* must also overcome host
69 defences to establish infection. *E. faecalis* can modulate and evade the host immune
70 response in a number of settings [21-24]. Biofilm formation, along with expression of the
71 SrtA substrate aggregation substance, can promote *E. faecalis* survival within

72 macrophages and polymorphonuclear leukocytes [25, 26]. The multiple peptide
73 resistance factor (MprF) protein of *E. faecalis* confers resistance to antimicrobial
74 peptides via electrostatic repulsion [27, 28], and is important for surviving both
75 neutrophil-mediated clearance and within epithelial cells and macrophages by a variety
76 of Gram-positive bacteria [29-31].

77 Previously, a mouse wound excisional model was developed to study wound healing
78 processes [32-34]. This model has been used to examine bacterial factors required for
79 wound infection by *Pseudomonas aeruginosa*, *Acinetobacter baumannii*, and
80 *Staphylococcus aureus* [35-38]. In the current study, we characterized the dynamics of
81 *E. faecalis* infection in the murine wound excisional model. We establish the minimal
82 doses of *E. faecalis* required for colonization and infection of wounds. We also
83 demonstrate a role for the innate immune defense factor MprF in wound infection, and
84 show that modulation of early inflammatory responses and delayed wound healing are
85 coupled with persistence of *E. faecalis* within wounds.

86 MATERIALS AND METHODS

87 Bacterial strains and growth conditions

88 Strains used are shown in Supplementary Table 1. For mouse infections, *E. faecalis*
89 were grown statically at 37°C for 15 to 18 hours in Brain Heart Infusion (BHI) medium
90 (Neogen, Lansing, USA) in the absence of antibiotics. Clinical strains isolated from
91 patient wounds were provided by Tan Tock Seng Hospital, Singapore.

92 Genetic manipulation

93 Construction of *E. faecalis* OG1RF $\Delta mprF1$ and $\Delta mprF2$ were previously described [27].
94 OG1RF $\Delta mprF1/2$ was made by subcloning the $\Delta mprF1$ deletion construct from
95 pJRS213- $\Delta mprF1$ into pGCP213 to create pGCP213- $\Delta mprF1$ and then transforming the
96 plasmid into OG1RF $\Delta mprF2$. Chromosomal deletions were selected for and screened
97 as described previously. Mutants $\Delta ebpABC$ and $\Delta srtAC$ are listed in Supplementary
98 Table 1.

99 Mouse wound excisional model

100 Mouse wound infections were modified from a previous study [39]. Male wild-type
101 C57BL/6 mice (7-8 weeks old, 22 to 25g; InVivos, Singapore) were anesthetized with
102 3% isoflurane and the dorsal hair trimmed. Following trimming, Nair™ cream (Church
103 and Dwight Co, Charles Ewing Boulevard, USA) was applied and the fine hair removed
104 via shaving with a scalpel. The skin was then disinfected with 70% ethanol. A 6-mm
105 biopsy punch (Integra Miltex, New York, USA) was used to create a full-thickness
106 wound and 10 μ l of the respective bacteria inoculum applied. The wound site was then
107 sealed with a transparent dressing (Tegaderm™ 3M, St Paul Minnesota, USA). At the

108 indicated time points, mice were euthanized and a 1 cm by 1 cm squared piece of skin
109 surrounding the wound site was excised and collected in sterile 1X PBS. Skin samples
110 were homogenized and the viable bacteria enumerated by plating onto both BHI plates
111 and antibiotic selection plates to ensure all recovered colony forming units (CFU)
112 correspond to the inoculating strain.

113 Histology

114 Wound tissues were excised as described above and fixed in 4% paraformaldehyde in
115 1x PBS (pH 7.2) for 24 hours at 4°C. Samples were then submerged in 15% and 30%
116 sucrose gradient for 24 hours each, embedded in Optimal Cutting Temperature (OCT)
117 embedding media (Sakura, California, USA), and frozen in liquid nitrogen. 10 µm thin
118 sections were then obtained with a Leica CM1860 UV cryostat (Leica Biosystems,
119 Ernst-Leitz Strasse, Germany) and stained with hemotoxylin and eosin (H&E). Images
120 of H&E sections were acquired using an Axio Scan.Z1 slide scanner (Carl Zeiss,
121 Göttingen, Germany) fitted with a 20x Apochrome objective.

122 Gene probe and Fluorescence *in-situ* Hybridization (FISH)

123 Detection of *E. faecalis* was achieved with the oligonucleotide probe 5'-GGT GTT GTT
124 AGC ATT TCG/Cy3/-3' (IDT Technologies, Iowa, United States). The general
125 oligonucleotide probe 5'- GCT GCC TCC CGT AGG AGT/Alexa Fluor® 488/-3' (IDT
126 Technologies, Iowa, United States) was used as a counterstain and targets the 16S
127 rRNA of organisms in the domain of *Bacteria* [40]. Cryo-sectioned tissue sections were
128 dehydrated in a graded ethanol series (70% and 80%) for 3 minutes each. Tissue
129 sections were then immersed in a 0.2% Sudan Black solution (prepared in 96% ethanol)

130 for 20 minutes and washed thrice with a 0.02% Tween solution (prepared in 1X PBS). A
131 total of 25 µl of 25% formamide hybridization buffer (20 mM Tris-HCl [pH 8.0], 5M NaCl,
132 0.1% sodium dodecyl sulfate, and 25% formamide) containing 100 pmol of the labelled
133 probe (50 µg/ml stock) was added to the sections and incubated overnight at 48°C.
134 Slides were then immersed in 50 ml of wash buffer (0.5M EDTA and 5M NaCl, 20mM
135 Tris-HCl [pH 8.0]) for 30 minutes in a 46°C water bath. After washing, slides were
136 plunged into ice cold water for 5 seconds and left to dry.

137 Confocal Laser Scanning Microscopy (CLSM)

138 Hybridized samples were mounted using Citifluor™ (Citifluor Ltd, Enfield Cloisters,
139 London) and imaged using an Elyra PS.1 LSM780 inverted laser scanning confocal
140 microscope (Carl Zeiss, Göttingen, Germany) fitted with a 63x/1.4 Plan-Apochromat oil
141 immersion objective using the Zeiss Zen Black 2012 SP2 software suite. Laser power
142 and gain were kept constant between experiments.

143 Scanning Electron Microscopy

144 Excised skin samples were fixed using 2.5% glutaraldehyde (prepared in 0.1M PBS pH
145 7.4) for 48 hours at 4°C and then washed three times with 0.1M PBS. Fixed samples
146 were then dehydrated with a graded ethanol series (once with 30%, 50%, 70%, 80%,
147 90% and twice with 100% for 15 minutes at each step) together with gentle agitation.
148 Samples were then subjected to amyl acetate immersion for 30 minutes. Samples were
149 next critical point dried with the Bal-Tec CPD-030 Critical Point Dryer (Bal-Tec AG,
150 Balzers, Liechtenstein) overnight and deposited onto SEM specimen stubs using NEM
151 Tape (Nisshin Em. Co. Ltd, Tokyo, Japan). Samples were then sputter coated with gold

152 using a Bal-Tec SCD 005 sputter coater (Bal-Tec AG, Balzers, Liechtenstein). Samples
153 were viewed using a JSM-6360LV (JEOL, Tokyo, Japan) scanning electron microscope.

154 Cytokine Luminex MAP analysis

155 Luminex MAP analysis was performed using the Bio-Plex Pro™ Mouse Cytokine 23-
156 plex Assay (Bio-Rad, California, USA) as previously described [41].

157 Flow cytometry

158 Skin was cut into pieces and incubated in RPMI containing 10% serum, 0.2mg/ml
159 Collagenase IV (Roche, Basel, Switzerland) and 20000U/ml of DNase I (Roche, Basel,
160 Switzerland) for 1 hour at 37°C. Cells were then passed through a 19 G syringe and
161 filtered through a 100 µm cell strainer (BD Biosciences, New Jersey, USA) to obtain a
162 homogenous cell suspension which was stained with the following fluorochrome or
163 biotin-conjugated monoclonal antibodies (mAbs): mouse IA/IE (M5/114.15.2) (BD
164 Biosciences, New Jersey, USA); Ly6G (1A8), CD64 (X54-5/7.1), F4/80 (BM8), EpCAM
165 (G8.8) (Biolegend, San Diego, United States) and, CD45 (30F11), Ly6C (HK1.4), CD24
166 (M1/69), and CD11b (M1/70) (eBioscience, California, USA). Multi-parameter analyses
167 of cell suspensions were performed on a LSR II (BD Biosciences, San Jose, USA). Data
168 were analyzed with FlowJo software (TreeStar, Oregon, USA).

169 Statistical Analyses

170 Statistical analyses were performed with GraphPad Prism software (Version 6.05 for
171 Windows, California, United States). Comparison of weight and CFU titres were
172 performed using the non-parametric Kruskal-Wallis test with Dunn's multiple comparison
173 post-test with p values <0.05 deemed significant. Cytokine and flow cytometry

174 comparisons were performed using the Mann-Whitney U test. Principal component
175 analysis was done in R (Version 3.3.2) with the packages factoextra (Version 1.0.4) and
176 FactoMineR (Version 1.34).

177 Ethics statement

178 All procedures were approved and performed in accordance with the Institutional Animal
179 Care and Use Committee (IACUC) in Nanyang Technological University, School of
180 Biological Sciences (ARF SBS/NIEA0198Z).

181 RESULTS

182 The minimum colonization dose for *E. faecalis* in wounds is 10 CFU

183 To investigate the colonization and infection dynamics of *E. faecalis* OG1RF in wounds,
184 we first determined the colonization dose required to colonize 50% of excisional wounds
185 in C57BL/6 mice (CD₅₀). We examined a range of infection inocula, ranging from 10¹ to
186 10⁶ CFU, at 24 hours post inoculation (hpi) and determined the CD₅₀ to be 10¹ CFU
187 which resulted in 80% of the mice having recoverable CFU (**Fig 1**). The CD₉₀ was 10²
188 CFU. In general, we observed that the median recoverable CFU for all inocula at 24 hpi
189 was similar to the initial inoculum. At inocula of 10¹ and 10², we observed no visible,
190 macroscopic signs of inflammation (**Supplementary Fig 1**). By contrast, at 24 hpi,
191 inocula of 10⁶ resulted in visible, macroscopic inflammation with redness and
192 accompanied by presence of serous exudates at the wound site of all infected mice
193 (**Supplementary Fig 1**). Henceforth, we defined 10⁶ as the infectious dose (ID₉₀).
194 These findings suggest that the initial bacterial inoculum can result in wounds of two
195 different states: colonization or infection.

196 *E. faecalis* infection is associated with high titer persistence in wounds

197 To further investigate the differences between low-inoculum colonization and high-
198 inoculum infection dynamics, we inoculated mice with the CD₉₀ colonization dose of 10²
199 CFU, or the infection dose of 10⁶ CFU, and monitored the mice for 7 days post
200 inoculation (dpi). We observed that, regardless of the initial infection inoculum, viable
201 bacteria were recovered at all time points (24 hpi to 7 dpi). However, after a 10² CFU
202 inoculation, *E. faecalis* persisted at 10² CFU and only decreased at 7 dpi (**Fig 2A**). By

203 contrast, when mice were inoculated with 10^6 CFU, we observed a rapid increase to 10^8
204 CFU by 8 hpi, followed by a decrease at 3 dpi to 10^5 CFU which was maintained
205 throughout the course of the experiment (**Fig 2B**). Consistent with this, at inocula of 10^6 ,
206 we observed visible inflammation and wound exudates only at 8 and 24 hpi, which
207 resolved after 2 dpi (data not shown).

208 *E. faecalis* wound infection dynamics were not strain-specific because the clinical blood
209 isolate *E. faecalis* V583 [42] displayed similar infection kinetics to that of strain OG1RF
210 (**Fig 2 C,D**). In addition, clinical *E. faecalis* wound isolates inoculated at the infection
211 dose resulted in similar high titer wound infections at 8 hpi (**Supplementary Fig 2**).
212 Together, these results demonstrate and confirm that the initial inoculum can determine
213 the following states: colonization in the absence of increase *E. faecalis* titers and overt
214 inflammation, or infection associated with acute bacterial replication and overt
215 inflammation.

216 **MprF contributes to *E. faecalis* fitness during wound infection**

217 To determine *E. faecalis* factors involved in wound colonization and infection, we
218 examined the fitness of previously described biofilm factors as well as factors involved
219 in immune defense. In competitive infections, we found that an Ebp null mutant was as
220 fit as wild type OG1RF at 3 dpi, indicating that biofilm-associated Ebp was not important
221 for wound infection (**Supplementary Fig 3**). Similarly, a Δ srtAC double mutant strain
222 defective in biofilm formation, was not attenuated in fitness during coinfection
223 (**Supplementary Fig 3**). Because we observed overt inflammation after high dose *E.*
224 *faecalis* infection in wounds, we predicted that resistance to host immune killing may be
225 important for its survival. *E. faecalis* encodes two paralogues of MprF [27, 28]. To

226 address the contribution of these gene products to fitness in wounds, we co-infected
227 wild type *E. faecalis* OG1X with the $\Delta mprf1/2$ strain, and found that while OG1X always
228 outcompetes OG1RF to some degree (**Supplementary Fig 3**), the $\Delta mprf1/2$ mutant
229 was massively outcompeted during co-infection (**Fig 3**). For wild type coinfection
230 experiments, for reasons we do not yet understand, we observed bi-modality of OG1X
231 out-competition of OG1RF, such that in each experiment some mice had much higher
232 OG1X CFU than others. Together, these results suggest that traditional biofilm-
233 associated factors may be less important for *E. faecalis* wound infection than its ability
234 to resist immune defense mechanisms.

235 ***E. faecalis* forms microcolonies on the wound surface**

236 Since we observed marked changes in the CFU recovered from infected wounds over
237 time, we hypothesized that the spatial distribution of *E. faecalis* may also vary across
238 time during infection. To address this question, we performed scanning electron
239 microscopy (SEM) at 8 hpi and 3 dpi which represent the peak of infection and the onset
240 of stable colonization, respectively. At 8 hpi, we observed *E. faecalis* microcolonies on
241 infected wounds that appeared to be encased within a matrix, indicative of early biofilm
242 development (**Fig 4A**). By contrast, at 3 dpi we were unable to detect *E. faecalis* on the
243 surface of the wounds (**Fig 4B**). Since the CFU burden was still high at 3 dpi, we
244 reasoned that *E. faecalis* may instead be embedded within the tissue. To determine the
245 spatial localization of sub-superficial *E. faecalis* in 3 dpi wounds, we performed
246 fluorescence *in-situ* hybridization (FISH) on 3 dpi wound samples. Using FISH probes
247 specific for *E. faecalis*, we observed *E. faecalis* microcolonies at the wound edge (**Fig**
248 **5A,C**), and in the wound bed (**Fig 5B,C**). These results suggest that as *E. faecalis*

249 wound infection proceeds, the bacteria first appear as biofilm-like microcolonies that are
250 later encapsulated or internalized within the host tissues. We postulate that both
251 properties may contribute to protection from the host immune response and persistence
252 within wounds.

253 **High titer *E. faecalis* infection alters wound healing and delays wound closure**

254 Infection of wounds by *P. aeruginosa* and *S. aureus* correlate with delayed
255 reepithelization and wound healing [43, 44]. To determine whether *E. faecalis* similarly
256 affects wound healing, we performed histology on skin tissue obtained from wounds of
257 infected mice at 7 dpi. Hemotoxylin and eosin (H&E) staining revealed a hyper-
258 thickened epidermis, indicative of non-progressive wound healing, with delayed closure
259 in the infected tissues which was not seen in the wounded, mock-infected controls (**Fig**
260 **6A,B**). Moreover, we also observed large numbers of polymorphonuclear leukocytes in
261 H&E stained infected samples as late as 7 dpi as compared to mock-infected controls
262 (**Fig 6A**). In addition, granulation tissue, which is indicative of dermal healing, was not
263 properly formed in infected wounds, whereas healing was visible in mock-infected
264 controls (**Fig 6A,B**). Long term persistence of *E. faecalis* also resulted in delayed wound
265 closure (**Fig 6C**). These observations show that high titer *E. faecalis* infection negatively
266 affects the wound healing process and delays the onset of wound closure.

267 ***E. faecalis* can persist within wounds while escaping immune detection**

268 We next hypothesized that *E. faecalis* might escape host detection during wound
269 infection, contributing to its ability to persist and delay wound healing. Therefore, to
270 examine the host immune response to *E. faecalis* infection, we first performed cytokine,

271 growth factor and chemokine analysis on supernatants from wound homogenates
272 inoculated with either 10^2 or 10^6 CFU, or PBS. At both 8 hpi and 3 dpi, wounds
273 inoculated with 10^2 *E. faecalis* CFU had cytokine and growth factor levels similar to the
274 PBS controls (**Fig 7A,B**). By contrast, wounds infected with 10^6 CFU displayed
275 significantly higher levels of the inflammatory cytokine IL-1b, as well as growth
276 factors/chemokines CSF3, CXCL1, CCL2, CCL3 and CCL4 compared to the controls at
277 8 hpi (**Fig 7A, Supplementary Fig 4A**), when macroscopic inflammation was observed.
278 At 3 dpi, when *E. faecalis* wound titers resolved to 10^5 CFU (**Fig 2B**), we observed
279 significantly lower levels of IL-2, IL-5, IL-10, IL12-p70, CCL11, IFN- γ and CSF2
280 compared to both 10^2 CFU-inoculated and PBS mock-infected wounds (**Fig 7B,**
281 **Supplementary Fig 4B**). Reduced cytokine and chemokine levels during steady state
282 infection suggest that *E. faecalis* may modulate the host immune response in wounds to
283 promote persistence.

284 To gain further insight into the spectrum of soluble factors that were most associated
285 with *E. faecalis* immune modulation during infection, we performed principal component
286 analysis (PCA) (**Supplementary Fig 4C**). The PCA profiles of wounds infected with 10^6
287 CFU at 8 hpi and 3 dpi were distinct and clustered separately, confirming that high
288 inoculum infection results in a different inflammatory profile temporally (**Supplementary**
289 **Fig 4C**). Differences in IL-1 β , IL-2, IL-12p70 and CCL11 specifically explained the
290 variation between the PCA profiles and best represented differences between all
291 sample groups. Among these, IL-2, IL-12p70 and CCL11 were significantly decreased in
292 the 10^6 CFU infected group when compared to the mock-infected controls, suggesting

293 that downregulation of these cytokines in particular may be associated with an
294 attenuated immune response (**Supplementary Fig 4B**).

295 To complement the analysis of soluble immune effectors, we performed flow cytometry
296 to quantify the immune cell types present at the wound sites. At 1 dpi, only neutrophil
297 infiltration was significantly increased in the infected wound compared to mock-infected
298 controls (**Fig 7C**). Increased neutrophil infiltration correlates with the upregulation of
299 chemotactic chemokines at 8 hpi (**Fig 7A**). However, at 3 dpi, there were significantly
300 more neutrophils, monocytes, macrophages, and monocyte derived cells in the infected
301 wounds compared to and mock-infected wounds (**Supplementary Fig 6B**). Despite the
302 presence of significant immune infiltrates at 3 dpi, the *E. faecalis* bacterial burden in the
303 wounds persisted at $>10^5$ CFU.

304 Taken together, these data demonstrate that high titer inocula, resulting in high titer
305 wound infection, is associated with an acute inflammatory response concomitant with
306 the peak of infection. The resolution of acute high titer infection to a lower steady state
307 infection at 3 dpi corresponds both a suppression of cytokine and chemokine levels yet
308 the presence of immune cellular infiltrate, suggests a complex immunomodulatory
309 program that is insufficient to resolve acute *E. faecalis* wound infection.

310 **DISCUSSION**

311 Globally, SSIs affect 7% and 15% of hospitalized individuals in developed and in
312 developing countries, respectively [1]. SSIs can extend the average hospitalization of
313 patients by 5 to 17 days [1]. Despite the prevalence and clinical importance of *E.*
314 *faecalis* wound infections, we know nothing of its pathogenic mechanisms in this
315 infection setting. Here, we established a modified mouse wound excisional model to
316 study the infection dynamics of *E. faecalis* as a model for surgical site infections.

317 We show that acute high titer *E. faecalis* wound infection associated with $\geq 10^6$ CFU is
318 associated with a robust cellular host immune response and visible signs of
319 inflammation, along with delayed wound healing, whereas inflammation is suppressed
320 or absent in lower titer infections. Our observations are consistent with reports showing
321 that bacterial counts of $\geq 10^6$ perturbs healing in humans [45, 46]. However, despite an
322 early robust inflammatory response, *E. faecalis* can persist in the local wound site
323 regardless of the inoculum load.

324 Consistent with reports that most wound infections involve biofilms, we observe the
325 presence of microcolonies at the surface of *E. faecalis* infected wounds at 8 hpi.
326 However, a sortase null mutant, deficient in the surface display of a variety of biofilm-
327 associated factors, was not attenuated in wounds. Together, these findings suggest that
328 *E. faecalis* wound-associated microcolonies or biofilms require other bacterial or host
329 factors for their development, and that currently understood biofilm factors are not
330 required in this niche. Furthermore, we discovered that after 3 dpi, *E. faecalis* can be
331 found at both the wound bed and at the epidermal wound edge, suggesting that *E.*
332 *faecalis* reservoirs within host cells may promote persistence in this niche.

333 Importantly, we show that *E. faecalis* wound infection results in immunomodulation. At 3
334 dpi, IL-2, IL-12p70, and CCL11 levels were lower in infected wounds compared to
335 mock-infected wounds, suggesting active immune suppression at the cytokine and
336 chemokine level. However, we still observed significant immune cell infiltrate at 3 dpi,
337 indicating that immune modulation may be insufficient to limit a full inflammatory
338 response. Nevertheless, the pro-inflammatory cellular infiltrate was not able to clear *E.*
339 *faecalis* from the wounds. Thus, it is tempting to speculate that *E. faecalis* wound
340 infection includes an active immune evasion or immune suppression component, which
341 contributes to high titer infection and long-term persistence, leading to the development
342 of a chronic, non-healing wound. Further, even modest *E. faecalis*-mediated immune
343 suppression may provide an advantage for co-infecting organisms commonly found with
344 *E. faecalis* in polymicrobial wound infections [10, 39]. Given the widespread prevalence
345 of Enterococcal wound infections, further studies into factors that promote *E. faecalis*
346 pathogenesis in wounds and its consequences on wound healing are critical.

347 **FUNDING INFORMATION**

348 This work was supported by the National Research Foundation and Ministry of
349 Education Singapore under its Research Centre of Excellence Programme, by the
350 National Research Foundation under its Singapore NRF Fellowship programme (NRF-
351 NRFF2011-11), and by the Ministry of Education Singapore under its Tier 2 programme
352 (MOE2014-T2-1-129).

353

354 **CONFLICT OF INTEREST**

355 The authors declare no conflict of interest.

356

357 **CORRESPONDENCE**

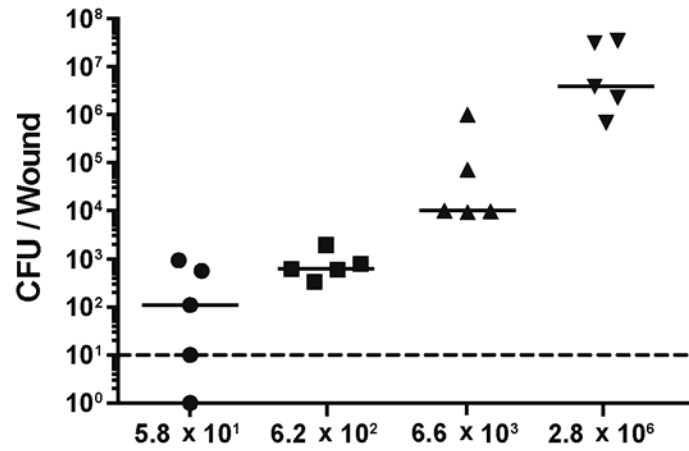
358 Kimberly Kline, Singapore Centre for Environmental Life Sciences Engineering,
359 Nanyang Technological University, SBS-B1n-27, 60 Nanyang Drive, Singapore 637551.
360 telephone: +65 6592 7943, fax: +65 6316 7349, kkline@ntu.edu.sg

361

362 **ACKNOWLEDGEMENTS**

363 We would like to thank Pei Yi Choo for her assistance with the FISH imaging. We would
364 also like to thank Milton Kwek and Declan Lunny for their help and advice regarding the
365 histology, sectioning, and staining of skin samples.

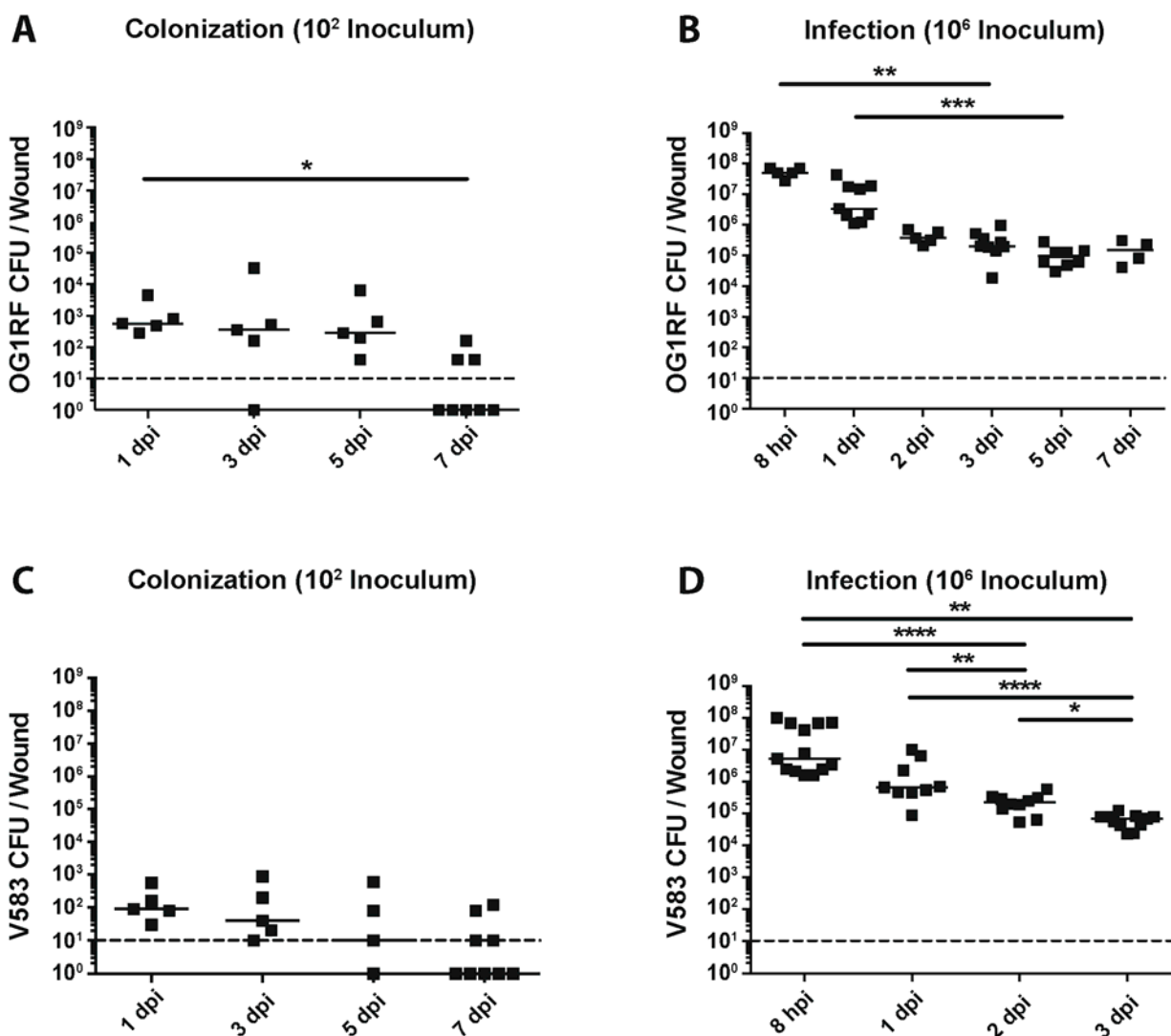
366 **FIGURES**



367

368 **Figure 1: The CD₅₀ of *E. faecalis* wound infection is 10¹ CFU.** Male C57BL/6 mice
369 were wounded and infected with *E. faecalis* OG1RF with an inocula of 10¹, 10², 10³ or
370 10⁶ colony forming units (CFU). Wounds were harvested at 24 hpi and the recovered
371 bacteria enumerated. Each dot represents one mouse, and the solid horizontal lines
372 indicate the median. The horizontal dashed line indicates the limit of detection, n=5.

373



374

375 **Figure 2: Colonization and infection dynamics of *E. faecalis* in wounds.** Wounds

376 were harvested at the indicated time points post-inoculation and the colony forming

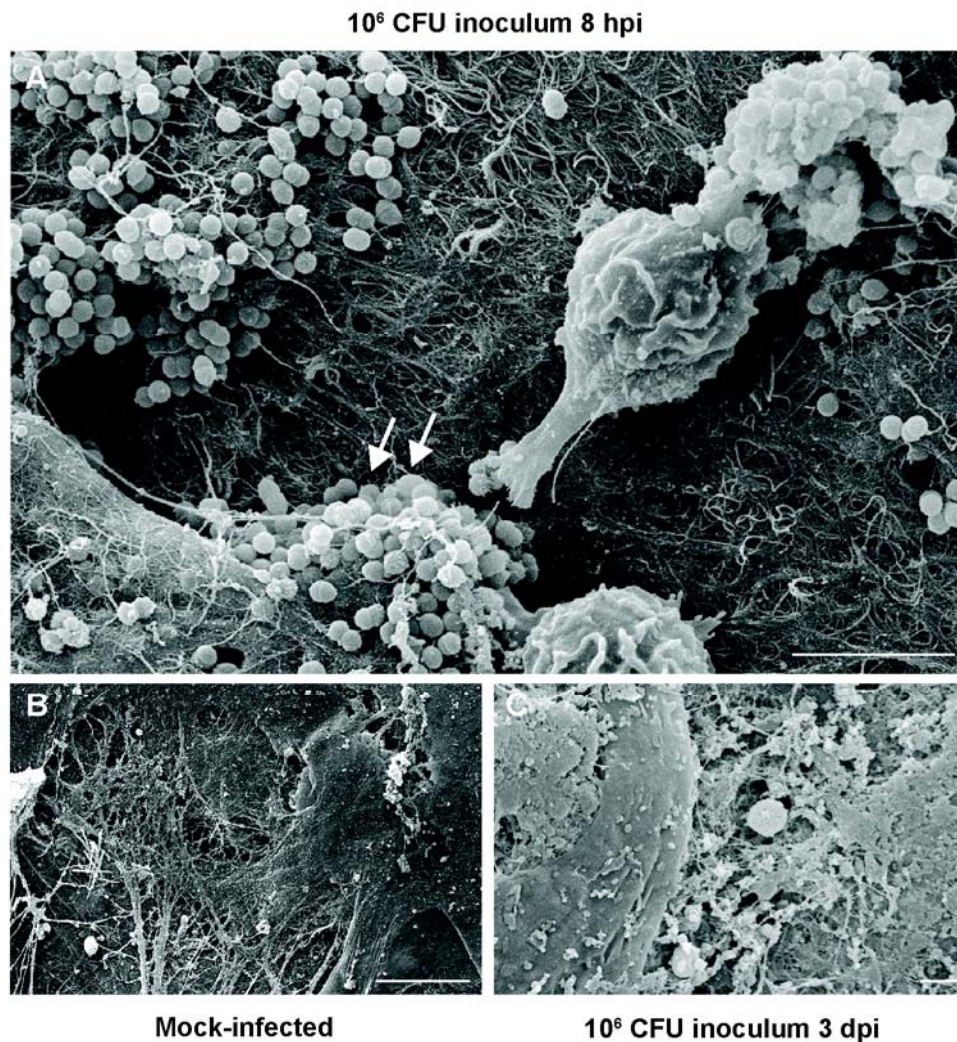
377 units (CFU) were enumerated. Mice were inoculated with **(A)** 10^2 CFU of OG1RF,

378 **(B)** 10^6 CFU of OG1RF, **(C)** 10^2 CFU of V583, or **(D)** 10^6 CFU of V583. Each dot

379 represents one mouse, and the solid horizontal lines indicate the median, $N=2$, $n \geq 5$.

380 Statistical analysis was performed using Kruskal-Wallis test with Dunn's post-test to

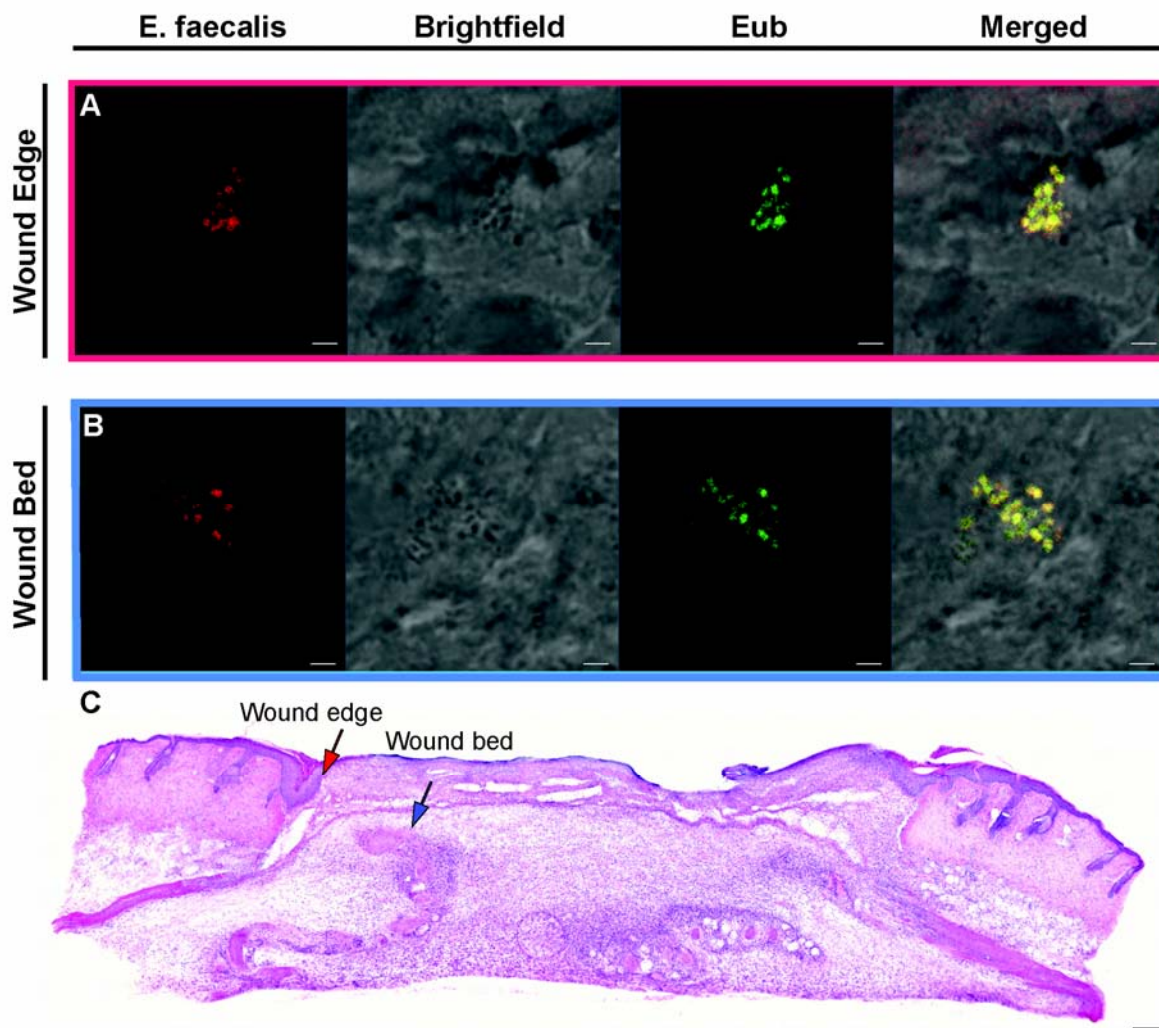
381 correct for multiple comparisons. * = $p < 0.05$, ** = $p < 0.01$.



392

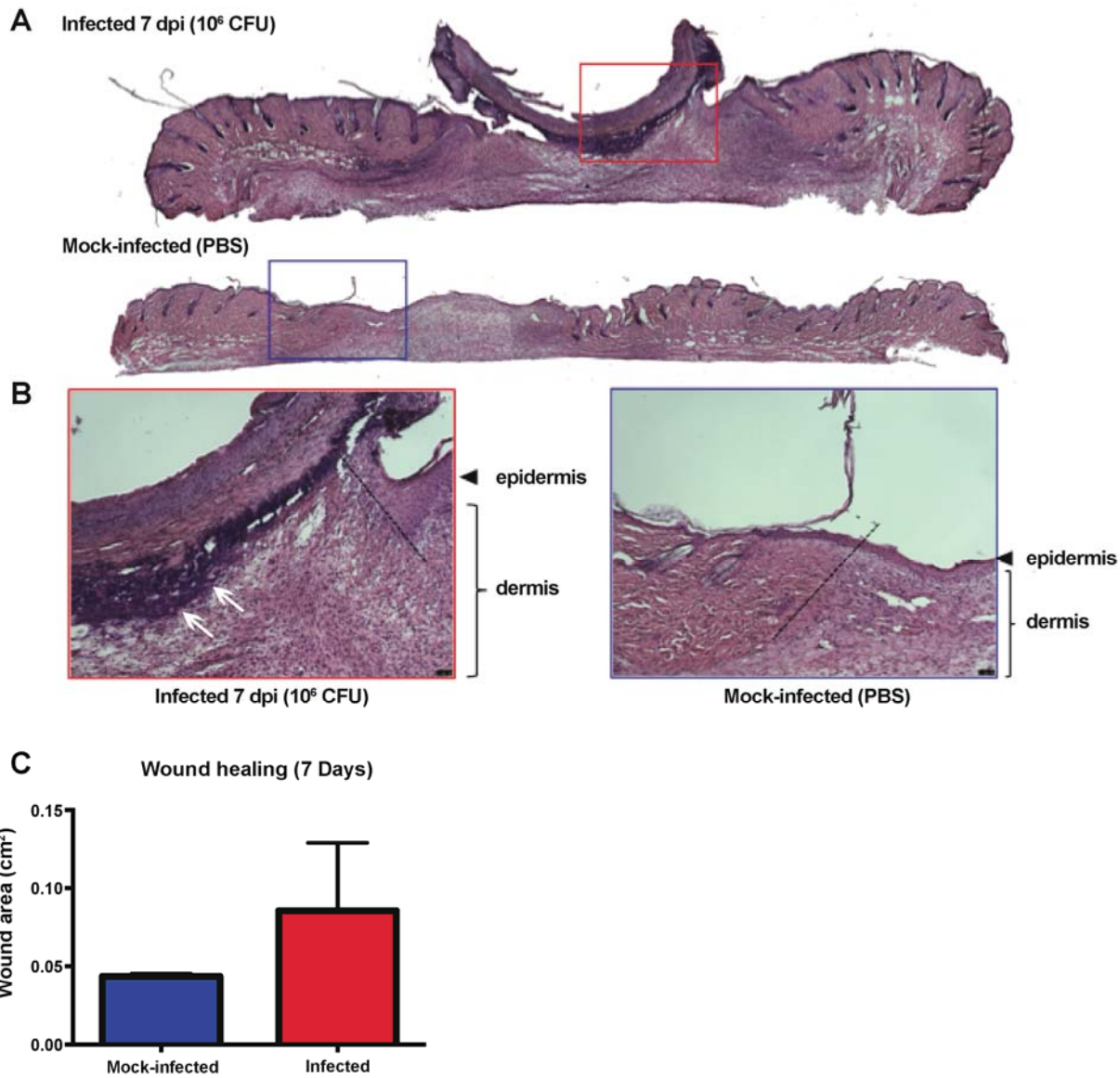
393 **Figure 4: *E. faecalis* forms microcolonies in acutely infected wounds.** Mice were
394 wounded and infected with 10⁶ CFU *E. faecalis* OG1RF or mock-infected with PBS.
395 Wounds were harvested at the indicated post-infection time points for scanning electron
396 microscopy. *E. faecalis* microcolonies encapsulated by fibrous material were visible at 8
397 hpi (white arrows, **A**), but not in mock-infected wounds (**B**) or in infected wounds at 3 dpi
398 (**C**). Bar represents 5 μm. Images shown are representative images from three
399 independent experiments.

400



401
402 **Figure 5: *E. faecalis* is present at the wound edge and in the wound bed.** Male
403 C57BL/6 mice were wounded and infected with 10^6 CFU of *E. faecalis* OG1RF. Wounds
404 were harvested at 3 days post-infection, cryosectioned, and subjected to (A,B) FISH or
405 (C) H&E staining. (A) *E. faecalis* specific probes or probes specific for the domain
406 bacteria (Eub) were used for FISH. The brightfield channel shows light microscopy
407 images. Red and blue arrows (C) correspond to the red and blue boxes (A,B) and
408 represent the wound edge and wound bed, respectively. (A,B) Bar represents 2 μ m.
409 Images shown are representative from three independent experiments.

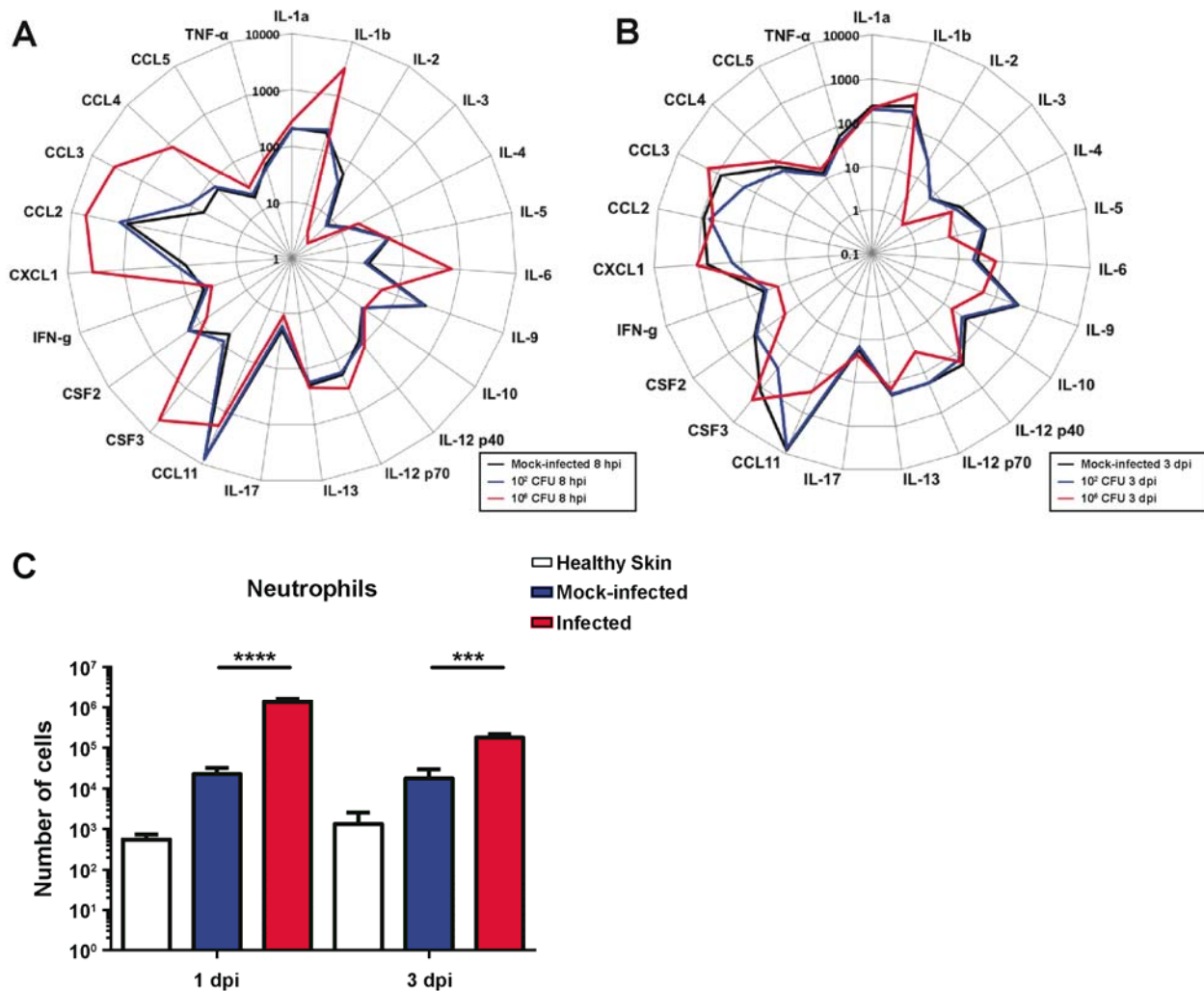
410



411

412 **Figure 6: *E. faecalis* infection alters wound healing dynamics.** Mice were wounded
413 and infected as described above. Wounds were harvested at 7 dpi and subjected to
414 H&E staining. **(A,B)** Red and blue boxes represent the wound edge for the infected
415 wounds and mock-infected controls, respectively. **(B)** Higher magnification images of
416 the boxes depicted in **A** and the dashed line indicate the wound edge. More clustered

417 polymorphonuclear leukocytes are present at the 7 dpi wound (white arrows) but absent
418 from the mock-infected wound. Bar represents 20 μ m. Images are representative
419 observations from three independent samples examined.
420



421
422 **Figure 7: *E. faecalis* modulates the soluble and cellular host response at the**
423 **wound site.** Mice were wounded and infected with 10² CFU or 10⁶ CFU of *E. faecalis*,
424 or mock-infected with PBS. At the indicated times, wounds were processed into single
425 cell suspensions and subjected to (A-B) cytokine analysis shown in pg/ml. (C) Total

426 number of neutrophils (CD45⁺ MHCII⁻ CD11b⁺ Ly6G⁺) infiltrating into and accumulating
427 in the skin analysed by flow cytometry during the immune response. N=2, n=5.
428 Statistical analysis was performed using Mann-Whitney U test comparing infected
429 against mock-infected wounds. * = $p < 0.05$, ** = $p < 0.01$, *** = $p < 0.001$, **** = $p <$
430 0.0001.

431 REFERENCES

- 432 1. WHO. Global Guidelines for the prevention of Surgical Site Infections. World Health Organisation
433 **2016**:184.
- 434 2. Dowd SE, Sun Y, Secor PR, et al. Survey of bacterial diversity in chronic wounds using pyrosequencing,
435 DGGE, and full ribosome shotgun sequencing. *BMC microbiology* **2008**; 8:43.
- 436 3. Bowler P, Duerden B, Armstrong D. Wound microbiology and associated approaches to wound
437 management. *Clinical microbiology reviews* **2001**; 14:244-69.
- 438 4. Giacometti A, Cirioni O, Schimizzi A, et al. Epidemiology and microbiology of surgical wound
439 infections. *Journal of clinical microbiology* **2000**; 38:918-22.
- 440 5. System NNIS. National Nosocomial Infections Surveillance (NNIS) System Report, data summary from
441 January 1992 through June 2004, issued October 2004. *American journal of infection control* **2004**;
442 32:470.
- 443 6. Gjødsbøl K, Christensen JJ, Karlsmark T, Jørgensen B, Klein BM, Krogfelt KA. Multiple bacterial species
444 reside in chronic wounds: a longitudinal study. *International wound journal* **2006**; 3:225-31.
- 445 7. Hollenbeck BL, Rice LB. Intrinsic and acquired resistance mechanisms in enterococcus. *Virulence* **2012**;
446 3:421-569.
- 447 8. Hurlow J, Couch K, Laforet K, Bolton L, Metcalf D, Bowler P. Clinical biofilms: a challenging frontier in
448 wound care. *Advances in wound care* **2015**; 4:295-301.
- 449 9. Metcalf DG, Bowler PG. Biofilm delays wound healing: A review of the evidence. *Burns & Trauma*
450 **2015**; 1:5.
- 451 10. Tay WH, Chong KKL, Kline KA. Polymicrobial–Host Interactions during Infection. *Journal of molecular*
452 *biology* **2016**.
- 453 11. Hall-Stoodley L, Stoodley P. Evolving concepts in biofilm infections. *Cellular microbiology* **2009**;
454 11:1034-43.
- 455 12. Kline KA, Kau AL, Chen SL, et al. Mechanism for sortase localization and the role of sortase
456 localization in efficient pilus assembly in *Enterococcus faecalis*. *Journal of bacteriology* **2009**; 191:3237-
457 47.
- 458 13. Nielsen HV, Flores-Mireles AL, Kau AL, et al. Pilin and sortase residues critical for endocarditis-and
459 biofilm-associated pilus biogenesis in *Enterococcus faecalis*. *Journal of bacteriology* **2013**; 195:4484-95.
- 460 14. Nallapareddy SR, Singh KV, Sillanpää J, et al. Endocarditis and biofilm-associated pili of *Enterococcus*
461 *faecalis*. *The Journal of clinical investigation* **2006**; 116:2799-807.
- 462 15. Nielsen HV, Guiton PS, Kline KA, et al. The metal ion-dependent adhesion site motif of the
463 *Enterococcus faecalis* EbpA pilin mediates pilus function in catheter-associated urinary tract infection.
464 *MBio* **2012**; 3:e00177-12.
- 465 16. Flores-Mireles AL, Pinkner JS, Caparon MG, Hultgren SJ. EbpA vaccine antibodies block binding of
466 *Enterococcus faecalis* to fibrinogen to prevent catheter-associated bladder infection in mice. *Science*
467 *translational medicine* **2014**; 6:254ra127-254ra127.
- 468 17. Nallapareddy SR, Qin X, Weinstock GM, Höök M, Murray BE. *Enterococcus faecalis* adhesin, ace,
469 mediates attachment to extracellular matrix proteins collagen type IV and laminin as well as collagen
470 type I. *Infection and immunity* **2000**; 68:5218-24.
- 471 18. Süßmuth SD, Muscholl-Silberhorn A, Wirth R, Susa M, Marre R, Rozdzinski E. Aggregation substance
472 promotes adherence, phagocytosis, and intracellular survival of *Enterococcus faecalis* within human
473 macrophages and suppresses respiratory burst. *Infection and immunity* **2000**; 68:4900-6.
- 474 19. Dunny GM, Leonard B, Hedberg PJ. Pheromone-inducible conjugation in *Enterococcus faecalis*:
475 interbacterial and host-parasite chemical communication. *Journal of bacteriology* **1995**; 177:871.

- 476 20. Shankar V, Baghdayan AS, Huycke MM, Lindahl G, Gilmore MS. Infection-derived *Enterococcus*
477 *faecalis* strains are enriched in *esp*, a gene encoding a novel surface protein. *Infection and immunity*
478 **1999**; 67:193-200.
- 479 21. Varahan S, Iyer VS, Moore WT, Hancock LE. *Eep* confers lysozyme resistance to *Enterococcus faecalis*
480 via the activation of the extracytoplasmic function sigma factor *SigV*. *Journal of bacteriology* **2013**;
481 195:3125-34.
- 482 22. Thurlow LR, Thomas VC, Fleming SD, Hancock LE. *Enterococcus faecalis* capsular polysaccharide
483 serotypes C and D and their contributions to host innate immune evasion. *Infection and immunity* **2009**;
484 77:5551-7.
- 485 23. Zou J, Shankar N. *Enterococcus faecalis* infection activates phosphatidylinositol 3-kinase signaling to
486 block apoptotic cell death in macrophages. *Infection and immunity* **2014**; 82:5132-42.
- 487 24. Park SY, Shin YP, Kim CH, et al. Immune evasion of *Enterococcus faecalis* by an extracellular
488 gelatinase that cleaves C3 and iC3b. *The Journal of Immunology* **2008**; 181:6328-36.
- 489 25. Baldassarri L, Bertuccini L, Creti R, et al. Glycosaminoglycans mediate invasion and survival of
490 *Enterococcus faecalis* into macrophages. *Journal of Infectious Diseases* **2005**; 191:1253-62.
- 491 26. Rakita RM, Vanek NN, Jacques-Palaz K, et al. *Enterococcus faecalis* bearing aggregation substance is
492 resistant to killing by human neutrophils despite phagocytosis and neutrophil activation. *Infection and*
493 *immunity* **1999**; 67:6067-75.
- 494 27. Kandaswamy K, Liew TH, Wang CY, et al. Focal targeting by human β -defensin 2 disrupts localized
495 virulence factor assembly sites in *Enterococcus faecalis*. *Proceedings of the National Academy of*
496 *Sciences* **2013**; 110:20230-5.
- 497 28. Bao Y, Sakinc T, Laverde D, et al. Role of *mprF1* and *mprF2* in the pathogenicity of *Enterococcus*
498 *faecalis*. *PLoS One* **2012**; 7.
- 499 29. Camejo A, Buchrieser C, Couvé E, et al. In vivo transcriptional profiling of *Listeria monocytogenes* and
500 mutagenesis identify new virulence factors involved in infection. *PLoS Pathog* **2009**; 5:e1000449.
- 501 30. Peschel A, Jack RW, Otto M, et al. *Staphylococcus aureus* resistance to human defensins and evasion
502 of neutrophil killing via the novel virulence factor *MprF* is based on modification of membrane lipids
503 with l-lysine. *Journal of Experimental Medicine* **2001**; 193:1067-76.
- 504 31. Thedieck K, Hain T, Mohamed W, et al. The *MprF* protein is required for lysinylation of phospholipids
505 in listerial membranes and confers resistance to cationic antimicrobial peptides (CAMPs) on *Listeria*
506 *monocytogenes*. *Molecular microbiology* **2006**; 62:1325-39.
- 507 32. Kirchner LM, Meerbaum SO, Gruber BS, et al. Effects of vascular endothelial growth factor on wound
508 closure rates in the genetically diabetic mouse model. *Wound repair and regeneration* **2003**; 11:127-31.
- 509 33. Cross S, Naylor L, Coleman R, Teo T. An experimental model to investigate the dynamics of wound
510 contraction. *British journal of plastic surgery* **1995**; 48:189-97.
- 511 34. Stiernberg J, Norfleet AM, Redin WR, Warner WS, Fritz RR, Carney DH. Acceleration of full-thickness
512 wound healing in normal rats by the synthetic thrombin peptide, TP508. *Wound repair and regeneration*
513 **2000**; 8:204-15.
- 514 35. Turner KH, Everett J, Trivedi U, Rumbaugh KP, Whiteley M. Requirements for *Pseudomonas*
515 *aeruginosa* acute burn and chronic surgical wound infection. **2014**.
- 516 36. Thompson MG, Black CC, Pavlicek RL, et al. Validation of a novel murine wound model of
517 *Acinetobacter baumannii* infection. *Antimicrobial agents and chemotherapy* **2014**; 58:1332-42.
- 518 37. Watters C, DeLeon K, Trivedi U, et al. *Pseudomonas aeruginosa* biofilms perturb wound resolution
519 and antibiotic tolerance in diabetic mice. *Medical microbiology and immunology* **2013**; 202:131-41.
- 520 38. DeLeon S, Clinton A, Fowler H, Everett J, Horswill AR, Rumbaugh KP. Synergistic interactions of
521 *Pseudomonas aeruginosa* and *Staphylococcus aureus* in an in vitro wound model. *Infection and*
522 *immunity* **2014**; 82:4718-28.

- 523 39. Keogh D, Tay WH, Ho YY, et al. Enterococcal Metabolite Cues Facilitate Interspecies Niche
524 Modulation and Polymicrobial Infection. *Cell host & microbe* **2016**; 20:493-503.
- 525 40. Kempf VA, Trebesius K, Autenrieth IB. Fluorescent in situ hybridization allows rapid identification of
526 microorganisms in blood cultures. *Journal of clinical microbiology* **2000**; 38:830-8.
- 527 41. Rousseau M, Goh HMS, Holec S, et al. Bladder catheterization increases susceptibility to infection
528 that can be prevented by prophylactic antibiotic treatment. *JCI Insight* **2016**; 1.
- 529 42. Bourgogne A, Garsin DA, Qin X, et al. Large scale variation in *Enterococcus faecalis* illustrated by the
530 genome analysis of strain OG1RF. *Genome biology* **2008**; 9:R110.
- 531 43. Goldufsky J, Wood SJ, Jayaraman V, et al. *Pseudomonas aeruginosa* uses T3SS to inhibit diabetic
532 wound healing. *Wound Repair and Regeneration* **2015**.
- 533 44. Schierle CF, De la Garza M, Mustoe TA, Galiano RD. Staphylococcal biofilms impair wound healing by
534 delaying reepithelialization in a murine cutaneous wound model. *Wound repair and regeneration* **2009**;
535 17:354-9.
- 536 45. Bendy Jr R, Nuccio P, Wolfe E, et al. Relationship of quantitative wound bacterial counts to healing of
537 Decubiti: Effect of topical Gentamicin. *Antimicrobial agents and chemotherapy* **1963**; 10:147-55.
- 538 46. Robson MC, Heggers JP. Delayed wound closures based on bacterial counts. *Journal of surgical*
539 *oncology* **1970**; 2:379-83.
- 540 47. Dunny GM, Brown BL, Clewell DB. Induced cell aggregation and mating in *Streptococcus faecalis*:
541 evidence for a bacterial sex pheromone. *Proceedings of the National Academy of Sciences* **1978**;
542 75:3479-83.
- 543 48. Sahm DF, Kissinger J, Gilmore M, et al. In vitro susceptibility studies of vancomycin-resistant
544 *Enterococcus faecalis*. *Antimicrobial Agents and Chemotherapy* **1989**; 33:1588-91.
- 545 49. Dunny GM, Craig RA, Carron RL, Clewell DB. Plasmid transfer in *Streptococcus faecalis*: production of
546 multiple sex pheromones by recipients. *Plasmid* **1979**; 2:454-65.